JPET Fast Forward. Published on February 26, 2004 as DOI: 10.1124/jpet.103.062802

Glucose-dependent enhancement of spontaneous phasic contraction is suppressed in diabetic mouse portal vein:

Association with diacylglycerol-protein kinase C pathway

***Koji Nobe, Hikaru Suzuki, Yasushi Sakai, Hiromi Nobe, Richard J. Paul & Kazutaka Momose**

Department of Pharmacology, School of Pharmaceutical Sciences (K.N., H.S., H.N. and K.M.), Division of Physiology, Department of Occupational Therapy, School of Nursing and Rehabilitation Sciences (Y.S.), Showa University, Tokyo 142-0555, Japan and Department of Molecular and Cellular Physiology, University of Cincinnati College of Medicine, Cincinnati OH 45267-0576, USA (R.J. P.)

JPET Fast Forward. Published on February 26, 2004 as DOI: 10.1124/jpet.103.062802
This article has not been copyedited and formatted. The final version may differ from this version.

Running title page

a) Runnning Title: Reduction of high glucose-dependent portal vein contraction

b) * Address correspondence to:

Koji Nobe, Ph.D., Department of Pharmacology,

School of Pharmaceutical Sciences, Showa University,

1-5-8 Hatanodai, Shinagawa-ku, Tokyo 142-0555, Japan

Tel: +81-3-3784-8212

Fax: +81-3-3784-3232

E-mail: kojinobe@pharm.showa-u.ac.jp

2) Counts

Text page: 34 (38) pages

Number of tables: 3

Number of figures: 7

Number of references: 31

Number of words in abstract: 205 words

Number of words in introduction: 576 words

Number of words in discussion: 1872 words

3) List of non-standard abbreviations

DG, diacylglycerol; HG-PSS, high glucose physiological salt solution; IDDM, insulin-dependent diabetes mellitus; NIDDM, non-insulin-dependent diabetes mellitus; OGTT, oral glucose tolerance test; PI, phosphatidylinositol; PMA, Phorbol-myristate acetate; PKC, protein kinase C; PLC, phospholipase C; PSS, physiological salt solution; PV, portal vein; TXA_2, thromboxan A_2.

4) Recommended section

Cardiovascular

JPET Fast Forward. Published on February 26, 2004 as DOI: 10.1124/jpet.103.062802
This article has not been copyedited and formatted. The final version may differ from this version.

ABSTRACT

We investigated portal vein (PV) contractility in diabetes using a mouse model (*ob/ob* mouse) of spontaneous non-insulin dependent diabetic mellitus. Spontaneous phasic contraction in control mice (C57Bl) was increased in the presence of the thromboxane A_2 analogue, U46619 in a time- and concentration-dependent manner. This response was enhanced under high glucose conditions (22.2 mM). Diacylglycerol (DG) was synthesized from glucose and was not affected by phospholipase C (PLC) inhibition under resting conditions in normal glucose. Inhibition of DG-induced PKC activation with Gö6976, a calcium-dependent protein kinase C (PKC) inhibitor, was only observed under normal glucose conditions. High glucose levels enhanced PLC-independent DG formation followed by an induction of total phosphatidylinositol (PI) turnover via calcium-independent PKC activation in C57Bl mice. In *ob/ob* mice, the high glucose-induced enhancement of PV contraction in response to U46619 was suppressed. These findings suggest that these differences are associated with long-term exposure of tissue to a hyperglycemic state. Under high glucose conditions, DG derived from glucose fell below 50% in C57Bl mice. Moreover, the DG-related calcium-independent PKC was desensitized in *ob/ob* mice. These results suggest that suppression of the glucose-induced enhancement of PV contraction involves both a decrease in glucose-derived DG formation and reduction of the glucose sensitivity of DG-related PKC.

JPET Fast Forward. Published on February 26, 2004 as DOI: 10.1124/jpet.103.062802
This article has not been copyedited and formatted. The final version may differ from this version.

Vascular dysfunction is a major complication in diabetes (Chaudhuri, 2002). Due to the reduced quality of life in these patients, alterations of vascular contractile responses in hyperglycemia have been investigated by many groups. It has been suggested that intracellular systems are altered in vascular tissue in diabetes (Ozturk et al., 1996). The relationships between hyperglycemia and smooth muscle dysfunction are important to furthering our understanding of diabetes; however, the mechanisms underlying these dysfunctions remain poorly understood.

In the two principal groups of diabetics, it is well known that treatment with insulin improves hyperglycemia as well as the dysfunction in vascular tissue in insulin-dependent diabetic mellitus (IDDM). Therefore, many types of insulin preparations have been used in IDDM patients. Despite the fact that the majority of diabetic patients have non-insulin-dependent diabetic mellitus (NIDDM), effective medicine and care for vascular complications have not been established. Dysfunction of vascular contractility in NIDDM is variable, dependent in part on the specific vessel (Chaudhuri, 2002). Thus an understanding of the dysfunction mechanisms in different vessels is necessary.

The portal vein (PV) functions as the main transfer vessel from the digestive organs to the liver. To effect a highly efficient transfer, the PV exhibits spontaneous intermittent rhythmic contractions (Miwa et al., 1997). Dysfunction of this tissue leads not only to reduction in blood supply to the liver but to serious diseases such as varix mediated by reflux of blood (MacMathuna, 1992). We previously reported that the magnitude of the spontaneous phasic contractions in mouse PV was increased in the presence of the thromboxane A_2 analog, U46619 (Nobe et al., 2003). We also reported that the U46619-induced contraction was significantly enhanced under high glucose conditions (twice the level of the normal conditions; 22.2 mM). We believe that the extracellular glucose-dependent enhancement of PV contraction might be associated with the variable blood glucose levels in PV as the blood originating from

JPET Fast Forward. Published on February 26, 2004 as DOI: 10.1124/jpet.103.062802
This article has not been copyedited and formatted. The final version may differ from this version.

digestive organs and the blood glucose levels depend on food intake and/or diabetic stage. An investigation of an intracellular signaling under high glucose conditions showed that the typical second messenger in phosphatidylinositol turnover (PI-turnover), diacylglycerol (DG), was significantly increased in U46619 stimulation. This DG increase paralleled cellular protein kinase C (PKC) activity suggesting that PKC activity accelerated a PI-turnover mediated by DG kinase activation (Kanoh et al., 1989; Nobe et al., 1997). Based on these findings, we hypothesized that this acceleration of PI-turnover contributed to the enhanced PV contraction. However, these studies were performed under short-term high glucose treatment of PV isolated from normal mouse (ddY mouse).

The results obtained from normal mouse PV treated with high glucose completely overlapped with the alterations observed in diabetes. In the present study, we investigated alterations of PV function in a spontaneous mouse model of NIDDM. The *ob/ob* mouse was selected for the NIDDM model as this homozygous strain is characterized by obesity, hyperglycemia, hyperinsulinemia and a blunted response to insulin at the receptor and postreceptor levels (Coleman and Hummel, 1967; Chang and Schneider, 1970; Vicario et al., 1987; Meyerovitch et al., 1989). These findings indicate that the *ob/ob* mouse is a suitable model for a human type NIDDM.

The objective of this investigation involve both detection of alteration of contractile responses in NIDDM mouse PV and elucidation of the intracellular mechanisms. Utilization of the *ob/ob* mouse PV revealed that enhancement of U46619-induced PV contraction under high glucose conditions was suppressed; furthermore, both decreased DG formation and glucose sensitivity of DG-dependent PKC were observed.

JPET Fast Forward. Published on February 26, 2004 as DOI: 10.1124/jpet.103.062802
This article has not been copyedited and formatted. The final version may differ from this version.

MATERIALS AND METHODS

Animals. Male C57Bl/6J obese mice (*ob/ob*) and their lean littermates (+/?; C57Bl) were purchased from Nippon Clea Corp. (Tokyo, Japan) at 5-8 wk of age. Mice were housed at constant room temperature (20 ± 2 ^{o}C) with 12 hr light and dark cycles. Mice were fed standard mouse chow, which included 5% fat (Oriental Yeast Corp., Tokyo, Japan). Food and water were available ad libitum and mice grew satisfactorily. At eight weeks of age, animals were used for experiments.

Oral Glucose Tolerance Test (OGTT). Mice were fasted overnight (12 hr) prior to the test. A basal glucose sample was obtained from each animal following administration of a 1 g/kg glucose solution by oral gavage. Blood samples were obtained at 10, 20, 30 and 60 min post gavage (Mathis et al., 2000). The glucose level in each sample was determined with a Tidex glucose analyzer (Bayer-Sankyo, Tokyo, Japan). Plasma immunoreactive insulin concentration was determined by radioimmunoassay using the polyethylene glycol method (Desbuquois and Aurbach, 1971). Blood samples were harvested in each type of mouse under 12 hr fasted conditions.

Measurement of Blood Cell Movement in Mouse PV. Mice were prepared in a manner identical to that of the OGTT procedure described above. Mice, which had been 12 h fasted (resting) and treated with glucose (1 g/Kg body weight, 30 min) mice were anesthetized with ether; subsequently, PVs were exposed. Blood cell movement in PV was measured with a non-contact type laser Doppler blood flow meter (Omega Co. Tokyo). Results were expressed as “% of resting level”.

Vessel Preparation. Mice were anesthetized with ether. PVs were dissected and prepared for analysis as previously described (Nobe et al., 2003). Briefly, vessels were rinsed in cold bicarbonate buffered physiological salt solution (PSS) and loose fat and connective tissue were removed. PSS, which contained (mmol/L): 137 NaCl, 4.73 KCl, 1.2 $MgSO_4$, 0.025 EDTA, 1.2 KH_2PO_4, 2.5 $CaCl_2$, 11.1 glucose

JPET Fast Forward. Published on February 26, 2004 as DOI: 10.1124/jpet.103.062802
This article has not been copyedited and formatted. The final version may differ from this version.

was buffered with 25.0 $NaHCO_3$; pH, when the solution was bubbled with 95% O_2 / 5% CO_2 was 7.4 at 37 ^oC. The endothelium was removed by gently rubbing the ring between the thumb and forefinger. The efficiency of endothelium removal via this method was confirmed histlogically as described previously; removal of the endothelium did not significantly affect the amount of force generated in response to NE administration (data not shown).

PV Force Measurements. PVs were mounted on a hook attached to an isometric force transducer (NEC San-ei Instruments Ltd., Tokyo, Japan). Optimal tension was established by adjustment of the length of the vessels to a point where maximum peak-to-peak oscillations of spontaneous isometric contractions were observed (Nobe et al., 2003). This passive tension was maintained throughout the experiment. Data, which were obtained utilizing Power Lab hardware, were analyzed employing Chart Software (AD Instruments Japan, Tokyo, Japan).

Measurement of Total Mass of DG. The total mass of DG in each tissue was measured in a manner similar to that described in a previously report (Nobe et al., 1993). Isolated tissues were treated under various conditions in 200 µL normal PSS or high glucose (HG-PSS). The reaction was terminated by addition of chloroform/methanol (1:2 by vol., 750 µL). Tissues were homogenized; subsequently, water and chloroform (200 µL of each) were added. The mixture was shaken followed by centrifugation at 1000×g. The lower phase was removed and dried under N_2 gas. The residue was redissolved in chloroform (concentration; 2 µl/mg wet weight tissue). This sample was spotted on a TLC plate (Merk, Silica gel 60 with concentrating zone). DG separation was effected with diethylether/heptane/acetic acid (75:25:1 by vol.). The plates were dried and stained with 0.03% of coomassie brilliant blue solution containing 30 % of methanol and 100 mM NaCl for 30 min; plates were distained for 5 min in dye-free staining solution. Each TLC plate was scanned; moreover, the density of each band was calculated using

JPET Fast Forward. Published on February 26, 2004 as DOI: 10.1124/jpet.103.062802
This article has not been copyedited and formatted. The final version may differ from this version.

NIH image software. Total mass of DG was determined from a dioreoyl-glycerol standard curve. Results were expressed as ng/mg wet weight tissue.

D-[^{14}C]glucose Incorporation into DG. Tissues were prelabeled with 33 mCi/ml D-[^{14}C]glucose containing normal- and HG-PSS at 37 ^{o}C for 60 min (Lee et al., 1989; Inoguchi et al., 1994). U46619 and/or additional reagents were introduced following this treatment. Following termination of these reactions, total lipids were extracted as described above. DG was separated on silica gel G thin-layer plates and developed in hexane/ether/acetic acid (60:40:1). Spots on the silica gel were removed by scraping; subsequently, radioactivity of [^{14}C]DG was measured on a liquid scintillation counter.

Measurement of Protein Kinase C (PKC) activity. Fresh tissues treated under various conditions were homogenized with a glass homogenizer in 0.5 mL of ice-cold solution consisting of 20 mM 3-(N-morpholino)propanesulfonic acid (MOPS) (pH 7.2), 250 mM sucrose, 1 mM dithiothreitol, 1 mM glycoletherdiaminetetraacetic acid (EGTA), 1 μg/mL pepstatin, 1 μg/mL leupeptin and 50 μg/mL trypsin inhibitor (Buffer A). The homogenates were centrifuged (1,000×g for 5 min) to remove the nuclei. Supernatants were decanted and pellets were washed once with buffer B (sucrose-free buffer A). The combined supernatants were centrifuged a second time (2,000×g for 30 min). Finally, the membrane and cytosol fractions were collected by centrifugation (100,000×g for 60 min). PKC activity in the membrane (pellet) fraction was determined utilizing an Amersham protein kinase C assay kit (Amersham Biosciences Japan, Tokyo, Japan).

Measurement of *myo*-inositol Incorporation. Measurement of *myo*-inositol incorporation was performed in a manner identical to the method of Conrad *et al*. (Conrad et al., 1991). [^{3}H]*myo*-inositol prelabeled tissues were preincubated in the presence or absence of each reagent for 10 min; subsequently, 100 nM U46619 was added for 5 min. Following termination of the treatment, incorporated [^{3}H]

JPET Fast Forward. Published on February 26, 2004 as DOI: 10.1124/jpet.103.062802
This article has not been copyedited and formatted. The final version may differ from this version.

phosphoinositides were analyzed.

Materials. [^{3}H]*myo*-inositol and D-[^{14}C]glucose were purchased from Du Pont-New England Nuclear (Boston, MA, U.S.A.). 9,11-dideoxy-11α, 9α-epoxymethanoprostaglandin $F_{2\alpha}$ (U46619), 12-(2-cyanoethyl)-6,7,12,13-tetrahydro-13-methyl-5-oxo-5H-indolo-(2, 3-α)pyrrolo(3,4-c)-carbazole (Gö6976), phorbol 12-myristate, 13-acetate (PMA) and 1-(6[([17β]-3-methoxyestra-1,3,5[10]-trien-17-ly)amino]hexyl)-1H-pyrrole-2,5-dione (U73122) were obtained from Sigma Chemical Co. (St. Louis, MO, U.S.A). Calphostin C and Mallotoxin (Rottlerin) were acquired from Calbiochem-Novabiochem Co. (San Diego, CA, U.S.A.). All other reagents, which were of the highest purity, were purchased from Sigma Chemical Co. (St. Louis, MO) except as noted. U46619 was dissolved in ethanol, whereas calphostin C, Gö6976 and PMA were dissolved in DMSO; no effects of vehicle were noted when total vehicle concentration was 0.03% or less.

Data Analysis. Values are presented as means ± SEM obtained from at least 5-16 animals. Statistical analyses for multiple comparisons were preformed using ANOVA for repeated measures followed by Student-Newman-Keuls (SNK) test in the cases depicted in Fig. 2-6. In the case of comparison with control (resting) response, repeated measures ANOVA followed by Dunnett's test was utilized (Table 1-3).

RESULTS

Basic Characteristics of the C57Bl and *ob/ob* mice. A significant increase in body weight (149.9%) was observed in the *ob/ob* mouse at 5-6 wks of age relative to C57Bl (Table 1). As typical of diabetes, changes in blood glucose levels during fasting and following food intake (OGTT; 1g/Kg body weight, 30 min) were also investigated. Following a 12 hr fast, blood glucose levels in *ob/ob* mice were

JPET Fast Forward. Published on February 26, 2004 as DOI: 10.1124/jpet.103.062802
This article has not been copyedited and formatted. The final version may differ from this version.

significantly higher than those in C57Bl mice (248.4% of C57Bl mice). OGTT led to increased glucose levels in C57Bl and *ob/ob* mice (144.8 % and 112.8 %, respectively); however, significant differences also remained. Insulin levels also increased in the *ob/ob* mice. Under conditions identical to those of OGTT, blood flow rate in PV was also examined (Table 2). After the 12 h fast (resting), blood cell movement in C57Bl mouse PV did not differ significantly from the corresponding value in *ob/ob* mice. This value was enhanced significantly by the OGTT (30 min) only in the C57Bl mouse. Blood cell movement was not influenced by glucose treatment in the *ob/ob* mouse. Direct treatment of 100 nM U46619 for PV significantly reduced blood cell movement in C57Bl and *ob/ob* mice.

U46619-induced Contractile Responses in Mouse PV. Spontaneous phasic contractile responses were observed in both C57Bl and *ob/ob* mouse PVs (Fig. 1). In the non-stimulated resting state, a force of 1.2 millinewtons (mN) was applied as a minimum resting tone. The absolute peak value of the spontaneous phasic contraction was 2.18 ± 0.01 mN (n=7). This response was maintained for at least 12 hr in our organ bath system (normal-PSS, pH 7.4, at 37^{o}C). These spontaneous contractions were detected in both types of mice.

In the C57Bl mouse PV, treatment with U46619 increased the peak force in a concentration-dependent manner (Fig. 1A-left). Stable responses were developed 3 min after U46619 addition. Significant increases in the peak responses from the resting state were initially detected at 3 nM U46619; the maximal value was obtained at 100 nM U46619 (3.54 ± 0.34 mN; n=7) and the EC_{50} value was 6.1 nM (n=7). This contractile response returned to resting levels in approximately 5 min following removal of U46619 via exchange of the bath contents. After the rinse, identical U46619-induced responses could be elicited (data not shown). Changes in phasic contraction were measured under high glucose conditions in the presence or absence of U46619 (Fig. 1A-right). Treatment of PV with PSS containing 22.2 mM

glucose (HG-PSS) for 30 min induced a slight increase in the peak values of the spontaneous contraction. Moreover, the increase in contractility elicited by U46619 was significantly augmented. Under high glucose conditions, 100 nM U46619 induced a maximal peak value of 4.38 ± 0.34 mN (n=7) and the EC_{50} value was 3.3 nM (n=7). Responses induced by U46619 under normal- and high-glucose conditions in C57Bl mice were similar to those previously described in the ddY mouse PV (Nobe et al., 2003).

In *ob/ob* mouse PV, both spontaneous contractions in the resting state and U46619-induced concentration-dependent increases were observed, which were similar to those of C57Bl mice (Fig. 1B-left). However, the enhancement of the contractile response was not observed under high glucose conditions (Fig. 1B-right). Maximal peak values of the contraction induced by 100 nM U46619 were 3.41 ± 0.25 and of 3.59 ± 0.33 mN (n=7), respectively. Incubation with HG-PSS for 12 hr did not restore the U46619 response (data not shown).

In order to assess the U46619-induced contractile response in normal- and HG-PSS, three parameters were extracted from the data presented in Fig.1 (Fig. 2). The following parameters were defined in our previous paper as follow (Nobe et al., 2003).

Amplitude. The "maximum-minimum" value in each phasic contraction was calculated. Results were expressed as an average in a 3-5 min window of stabilized response. Results were expressed in millinewtons (mN).

Frequency. The number of contractile events in a 3-5 min window of stabilized response was counted. Threshold consisted of 30% of each spontaneous response. Results were expressed in cycles per minute (cycles/min).

ON-time. Total seconds of force in excess of 20% of the maximal response induced by 100 nM U46619 in a 3-5 min window of stabilized response. Results were expressed as seconds per minute

JPET Fast Forward. Published on February 26, 2004 as DOI: 10.1124/jpet.103.062802
This article has not been copyedited and formatted. The final version may differ from this version.

(sec/min).

In the resting state of C57Bl mouse PV, the amplitude (minus the applied basal tension) was 0.98 ± 0.01 mN (n = 5). This amplitude increased in a manner dependent upon the U46619 concentration in C57Bl mice under normal conditions (Fig. 2A). Maximal values were detected with 10 nM U46619 (2.59 ± 0.16 mN; n = 5). Following attainment of maximal amplitude, the readings fell to 20 % of maximal values upon stimulation with 100 nM U46619. Under high glucose conditions, a similar pattern of change was observed. Although maximal amplitude accurred at 10 nM U46619 stimulation (5.33 ± 0.35 mN; n = 5), most values in HG-PSS were significantly larger than those in normal-PSS. In the *ob/ob* mice, the amplitude increased depending on the U46619 concentration, which was similar to the response in C57Bl mice. Significant differences between *ob/ob* and C57Bl mice were not evident under normal conditions. After the treatment with HG-PSS, enhancements of the amplitude relative to corresponding values in normal-PSS were detected at 6-30 nM U46619, however, the maximum enhancements were 44.2 % of corresponding values present in C57Bl mice. Significant differences between *ob/ob* and C57Bl mice in HG-PSS were observed during stimulation with 3-100 nM U46619 stimulation.

The correlation between frequency and ON-time was graphed in C57Bl mice (Fig. 2B). In the resting state, frequency and ON-time displayed readings of 2.11 ± 0.01 cycles/min and 16.5 ± 0.06 sec/min, respectively (n = 5). In a manner dependent on U46619 concentration, the frequency effectively increased relative to the ON-time values. Maximal frequency was detected during stimulation with 6 nM U46619 stimulation (3.02 ± 0.04 cycles/min). Subsequently, ON-time increased to maximal levels (60 sec/min). These results revealed that the relationship between frequency and ON-time changed in a counterclockwise manner. Under HG conditions, the relationship also exhibited counterclockwise changes; however, ON-time readings were significantly enhanced during stimulation with U46619.

During this period, frequency did not differ from those values present in normal-PSS. In *ob/ob* mice, similar counterclockwise changes in the relationship between frequency and ON-time were detected in normal PSS (Fig. 2C). Frequency and ON-time in the resting state displayed readings of 1.85 ± 0.01 cycles/min and 14.5 ± 0.01 sec/min, respectively (n = 5). Maximal frequency was detected during 6 nM U46619 stimulation (2.97 ± 0.02 cycles/min; n=5); furthermore, ON-time indicated submaximal values during stimulation with U46619 at levels in excess of 10 nM. These responses were similar to the corresponding values in C57Bl mice. This relationship was not affected following treatment with HG-PSS. Significant differences were not detected under these conditions.

Effects of long-term preincubation under normal and high glucose conditions on the U46619-induced increase in amplitude were investigated in C57Bl and *ob/ob* mouse portal veins (Fig. 3). During the preincubation (0.5-12 h), fresh normal and high glucose PSS were exchanged every 30 min, and both temperature (37^{o}C) and resting tension (1.2 mN) were maintained. After the incubation, 10 nM U46619 treated for 10 min and then amplitudes were calculated. The enhancements of high glucose-induced amplitude were detected during 0.5-12 hr preincubation in C57Bl mouse (5.28 ± 0.11 mN in 12 h incubation). In *ob/ob* mouse portal vein, incubation in normal PSS did not alter the amplitudes compared to high glucose PSS. Moreover, the high glucose induced enhancement of amplitude could not be detected at least for 12 hr incubation in high glucose PSS (2.30 ± 0.15 mN in 12 h incubation).

Alteration of Intracellular DG levels in Diabetic Mouse PV. In C57Bl mice, the endogenous DG level in the resting state was 149.2 ± 7.26 ng/mg wet weight (n=5) (Fig. 4). U46619 (100 nM) significantly elevated this level to 231.3 ± 10.6 ng/mg wet weight (n=5). In normal-PSS, the U46619-induced response was suppressed by pretreatment with the phospholipase C (PLC) inhibitor, U73122 (1

JPET Fast Forward. Published on February 26, 2004 as DOI: 10.1124/jpet.103.062802
This article has not been copyedited and formatted. The final version may differ from this version.

μM, 10 min) with no affect on resting levels. Under the HG conditions, the resting level of DG increased significantly to 248.5 ± 22.1 ng/mg wet weight (n=5). DG further increased to 294.2 ± 14.2 ng/mg wet weight (n=5) upon stimulation with 100 nM U46619. Treatment with U73122 in HG-PSS did not significantly affect the U46619-induced increases in the endogenous DG level. In *ob/ob* mice, resting and U46619-treated values of endogenous DG levels in normal-PSS were 149.7 ± 15.3 and 213.4 ± 14.7 ng/mg wet weight (n=5), respectively. These values were quite similar to the corresponding values in C57Bl mice. As in the case of C57Bl mice, pretreatment with HG-PSS enhanced resting and U46619-treated DG levels (204.0 ± 10.2 and 255.7 ± 8.6 ng/mg wet weight, respectively; n=5). Additionally, enhancement was not affected by the U73122 treatment. However, enhancement under HG-PSS in *ob/ob* mice was blunted, it was approximately 50 % of the enhancement observed in C57Bl mice.

To elucidate the association between high glucose treatment and endogenous DG formation, incorporation of [^{14}C]glucose into DG was measured (Table 3). In C57Bl mouse PV, formation of [^{14}C]DG was not significantly elevated by treatment with 100 nM U46619 in normal PSS. However, the formation in HG-PSS as well as in the resting state was significantly enhanced by U46619 treatment. These enhancements exceeded 200 % of the values in normal PSS. Under the HG-PSS, a U46619 induced increase in [^{14}C]DG formation was not detected. In *ob/ob* mice, [^{14}C]DG formation in normal PSS did not differ from the value in C57Bl mice. This value was not affected by the U46619 stimulation. Under high glucose conditions, [^{14}C]DG formation was also enhanced in resting and U46619 treated tissues; in contrast, the enhancements were approximately 140% of those values obtained in normal PSS. The increases under high glucose conditions were significantly smaller than those in C57Bl mice.

Alteration of PKC Activity in Diabetic Mice PV. In C57Bl mice, the PKC activity in the membrane fraction of the non-stimulated resting state was 5.84 ± 0.24 pmol/min/mg protein (n=5) (Fig.

5A). This activity increased significantly upon treatment of tissue with 100 nM U46619 (18.15 ± 0.88 pmol/min/mg protein; n=5). In order to detect the specific inhibitory effects of the PKC inhibitors, we measured the time- and dose-dependency of the inhibitors (data not shown). From these preliminary trials, each condition was adopted as minimum concentration in the critical inhibitory range. Pretreatment with U73122 (1 μM, 10 min) significantly reduced the U46619-induced PKC activation (24.2 % of U46619-induced activation). Both general types of PKC inhibitor (1 μM calphostin C) and a calcium-dependent PKC inhibitor (1 μM Gö6976) suppressed the U46619-induced PKC activation. In contrast, the calcium-independent PKC inhibitor, Rottlerin did not affect the responses. Moreover PKC activator (3 μM PMA) significantly enhanced the PKC activity in C57Bl mouse PV (19.15 ± 0.83 pmol/min/mg protein; n=5).

Similar trials were performed under high glucose conditions. In the non-stimulated resting state in HG-PSS, PKC activity in the membrane fraction (19.96 ± 1.01 pmol/min/mg protein; n=5) was significantly greater in comparison with the corresponding value in normal-PSS. This increase was maintained under U46619 stimulation (21.48 ± 0.89 pmol/min/mg protein; n=5); furthermore, it was not affected by pretreatment with U73122. Calphostin C and Rottlerin (1 μM, 5 min) reduced the PKC activity in HG-PSS; however, the effects were incomplete (11.48 ± 0.82 and 12.90 ± 0.76 pmol/min/mg protein; n=5). Moreover, Gö6976 did not influence the PKC activity. Under high glucose conditions, PMA induced PKC activation; however, the value was not different from the value observed under normal conditions.

In *ob/ob* mouse PV, resting activity of PKC in normal-PSS was similar to the value in C57Bl mice (Fig. 5B). PKC activity was 5.15 ± 0.28 pmol/min/mg protein (n=5). Treatment with U46619 enhanced the PKC activity in *ob/ob* mice (9.02 ± 0.30 pmol/min/mg protein; n=5). However, this U46619-induced

JPET Fast Forward. Published on February 26, 2004 as DOI: 10.1124/jpet.103.062802
This article has not been copyedited and formatted. The final version may differ from this version.

increase in PKC activity was significantly smaller than that in C57Bl mice (31.1% of the increase in C57Bl mice). PLC and PKC inhibitors suppressed the U46619-induced PKC activation. PMA also enhanced the PKC activity. However, this value also was significantly lower than that of C57Bl mice. Under high glucose conditions, the enhancement of resting PKC activity displayed in the C57Bl mouse was not detected (4.24 ± 0.50 pmol/min/mg protein; n=5). U46619 increased PKC activity; however, the activity did not exceed the corresponding level in normal PSS (7.47 ± 0.40 pmol/min/mg protein; n=5). Activation of PKC following U46619 treatment was not affected by U73122. A calcium-independent PKC inhibitor (Rottlerin) reduced the activation; on the other hand, Gö6976 exerted no affect on the response. Treatment with PMA failed to induce PKC activity under high glucose conditions in *ob/ob* mouse PV.

Acceleration of PI-turnover in Diabetic Mice PV. In order to determined the total PI-turnover activity, the incorporation of [^{3}H] *myo*-inositol in mouse PV was investigated (Fig. 6). Tissues were incubated with [^{3}H] *myo*-inositol under several conditions for 5 min; subsequently, intracellular [^{3}H] inositol-phospholipids were subsequently analyzed.

For the C57Bl mice in the resting state, the total mass of [^{3}H] *myo*-inositol incorporation was 2384 ± 187.7 cpm/mg wet weight tissue (n=5). This value was elevated significantly by 100 nM U46619 (7436 ± 655.8 cpm/mg wet weight tissue; n=5). Moreover, this response was suppressed by pretreatment of U73122 (3038 ± 254.1 cpm/mg wet weight tissue; n=5). On the other hand, treatment with HG-PSS significantly increased the resting levels of [^{3}H] *myo*-inositol incorporation (6994 ± 180.6 cpm/mg wet weight tissue; n=5). This increase was maintained by U46619 stimulation; moreover, it was not influenced by U73122 pretreatment.

For the *ob/ob* mouse PV, [^{3}H] *myo*-inositol incorporation in normal-PSS was similar to the

JPET Fast Forward. Published on February 26, 2004 as DOI: 10.1124/jpet.103.062802
This article has not been copyedited and formatted. The final version may differ from this version.

response in C57Bl mice. Resting and U46619 treated responses were 2756 ± 579.5 and 6186 ± 112.6 cpm/mg wet weight tissue (n=5), respectively. However, enhancement of the resting level in HG-PSS was not detected (2976 ± 238.0 cpm/mg wet weight tissue; n=5). Under high glucose conditions, U46619 increased the [^{3}H] *myo*-inositol incorporation (4026 ± 452.6 cpm/mg wet weight tissue; n=5); however, the value was significantly lower than that observed in C57Bl mice. The response was not affected by U73122 treatment as well. These values were not different from those readings obtained in normal-PSS. The inhibitory effects of U73122 were also detected in HG-PSS.

DISCUSSION

Our current results indicate that the dysfunction of PV contraction in the NIDDM mouse model involves both alteration of the conversion of glucose to DG and reduce of glucose dependency of DG-dependent PKC. The *ob/ob* mouse is characterized by obesity and other complications of diabetes (Meyerovitch et al., 1991). We also detected a marked increase in body weight in comparison with lean littermates (C57Bl mouse) as well as increases in blood glucose and insulin levels (Table 1). OGTT results confirmed that *ob/ob* mice display sustained hyperglycemia despite fasting and food intake. These findings were in agreement with previous research (Meyerovitch et al., 1991). PV isolated from *ob/ob* mice demonstrated spontaneous phasic contractions in the non-stimulated resting state (Fig. 1B). This response was indistinguishable from the response in C57Bl mice (Fig. 1A). Significant enhancement of U46619-induced contractions under high glucose conditions in C57Bl mouse PV (Fig. 1A) was similar to that observed in our previous study (Nobe et al., 2003). The patterns of increases in amplitude and ON-time and lack of effect on frequency were well correlated with the response in ddY mouse (Nobe et al., 2003). These results would suggest that the contractile response in C57Bl mice was elevated under high

JPET Fast Forward. Published on February 26, 2004 as DOI: 10.1124/jpet.103.062802
This article has not been copyedited and formatted. The final version may differ from this version.

glucose conditions, contributing to efficient blood cell movement (Table 2). We also confirmed the existence of 100 nM U46619-induced decreases in blood flow rate in PV. Why was the frequency unaffected? The basis for the minimal effects on frequency is unknown, largely due to an inadequate understanding of the regulatory mechanisms controlling this parameter.

In the *ob/ob* mouse PV, significant U46619-induced increases in the contractile response were detected (Fig. 1B); however, this increase was not influenced by the extracellular glucose concentration. Similar results were obtained after long-term preincubation of PVs in normal or high glucose PSS. The high glucose-induced enhancement of the contraction in the C75Bl mouse was maintained for at least 12 hr of incubation. The enhancement could not be detected in the *ob/ob* mouse after preincubation (12 hr) with normal PSS (Fig. 3). These results indicated that the U46619-induced PV contraction in the diabetic model was desensitized to extracellular glucose. The *ob/ob* mouse exhibited constitutive hyperglycemia (Table 1). Consequently, we believe that this reduction of the dependence on glucose is a chronic dysfunction and it is attributable to long-term exposure of the PV to hyperglycemia. It may lead to decreased blood provision to the liver as well as decreased blood flow at the PV. It could precede serious conditions such as stagnation and/or high portal pressure. Alteration of blood cell movement was also confirmed in Table 2. Elevation in PV contraction induced by 5-hydroxytryptamine stimulation were documented in Schistosoma mansoni-infected mice (Silva et al., 2003), however, the association of glucose level with PV contraction remains poorly understood.

The enhancement of PV contraction under high glucose conditions including increases in both amplitude and ON-time (Fig. 2) has been detected previously. Therefore, we suggested that the regulatory mechanisms governing these parameters might be disabled under diabetic conditions. To identify the regulation and dysfunction, intracellular signaling systems were examined. We previously

reported that the intracellular DG levels increased under high glucose conditions in ddY mouse PV (Nobe et al., 2003). Additionally, we suggested that this increase led to the enhancement of PV contraction mediated by an acceleration of PI-turnover. In the present study, the alteration of intracellular DG level and its synthesis pathways in C57Bl and *ob/ob* mice were investigated.

In the C57Bl mouse PV under normal glucose conditions, U46619 induced a significant increase in total mass of DG (Fig. 4). This DG formation derived from phosphatidylinositol hydrolysis mediated by PLC. However, the total mass of DG was sub-maximally enhanced under high glucose conditions in the absence of U46619 stimulation. We found that the enhanced DG level in HG-PSS was a consequence of glucose incorporation via the *de novo* synthesis pathway (Table 3). These results indicated that the increase in intracellular DG level was dependent on different synthesis pathways under normal or high glucose conditions (Scheme A). DG formation from glucose has been described in some cell types (Rossi et al., 1991). Furthermore, it was suggested that DG formation was enhanced in hyperglycemia (Lee et al., 1989). It was also reported that the side chain (two acyl-groups) conformation of DG was dependent on the formation route and that they play different roles (Dawson et al., 1984; Szule et al., 2002).

We hypothesized that the changes in the alteration of PV contractility under high glucose conditions may depend on which DG synthesis pathways were involved. To confirm this hypothesis, several downstream signal transduction pathways of DG were investigated. A major target of the DG signal is PKC. It is widely accepted that the DG-PKC signal pathway functions as a regulatory factor in vascular contraction (Lee and Severson, 1994). We measured PKC activities in PV membrane fractions (Fig. 5), attributable to the occurrence of DG as a membrane bound lipid. In the membrane fraction isolated from C57Bl mouse PV, PKC activities under conditions of resting and U46619 treatment were well correlated with the changes in total mass of DG (Fig. 4 & 5). Similar results were obtained in ddY

mouse PV (data not shown). Moreover, data demonstrated that U46619-induced PKC activation is calcium-dependent (Gö6976-sensitive) under normal glucose conditions, whereas calcium-independent (Rottlerin-sensitive) PKC was activated under high glucose conditions (Fig. 5A). Rottlerin possesses selectivity for PKCδ in vascular smooth muscle (Wakino et al., 2001); as a result, this isoform might play a role in PV contraction. These observations indicated the possibility that the activation of PKC isoforms was distinguishable under normal and high glucose conditions and furthermore, this situation may arise due to different origins of DG formation. Alterations of PKC activity under high glucose conditions have been noted in some groups (Babazono et al., 1998; Ganz and Seftel, 2000). We believe that this is the first report of different types of glucose-dependent activation of PKC associated with DG formation. In vascular tissue, PKC induces not only calcium sensitization but also accelerated PI-turnover mediated by activation of a specific component of the PI-turnover, i.e., phosphorylation of DG kinase (Kanoh et al., 1989; Nobe et al., 1995). Both mechanisms contribute to the increase in vascular contraction.

As a measure of the total activity of the PI-turnover under high glucose conditions, *myo*-inositol incorporation was measured (Fig. 6). This was enhanced by U46619 stimulation in normal PSS; moreover, PI-turnover was suppressed by inhibition of PLC. This situation was similar to the alteration of DG levels (Fig. 4). Under high glucose conditions, PI-turnover also accelerated in a manner that paralleled the changes in both DG and PKC activity without being affected by a calcium-dependent PKC inhibitor. These results indicated that the increased DG (derived from glucose) induced the PI-turnover acceleration was mediated by calcium-independent PKC activation. We suggest that enhancement of U46619-induced spontaneous contraction under high glucose conditions in C57Bl mouse PV involves the following steps: (1) an incorporation of glucose, (2) conversion to DG, (3) calcium-independent PKC activation and (4) PI-turnover acceleration (Scheme A). These physiological responses in PV contraction

likely function as a mechanism to enhance hepatic blood flow rate during transient increases in blood glucose levels.

We next investigated steps are altered in the PV response in the NIDDM mouse model. We next considered the intracellular factors which may underlie the suppression of enhancement of the U46619-induced contraction under high glucose conditions. The U46619-induced increase in total mass of DG was enhanced under high glucose conditions; however, the increase in this level was only slight in comparison with that observed in C57Bl mice (Fig. 4). Moreover, incorporation of [^{14}C]glucose into DG was also only a modest (approx. 40 % increases; Table 3). These results indicated that incorporation of glucose and/or conversion of the glucose to DG had been reduced in *ob/ob* mouse PV (Scheme 2). These phenomena agreed with the general observation that the reduction in the incorporation of glucose in NIDDM was mediated by insulin receptor desensitization (Pillay and Makgoba, 1991) and inactivation of glucose transporter (Khan and Pessin, 2002). We theorized that reduction of glucose incorporation and/or DG synthesis was a major cause of the suppression of enhancement of contraction under high glucose conditions in the *ob/ob* mice. However, enhancement of both DG level and [^{14}C]glucose incorporation under high glucose conditions in *ob/ob* mice remained at levels that were approximately 50% of corresponding levels observed in C57Bl mice. Under the identical conditions, however, the high glucose-induced increases in amplitude and ON-time were, however, suppressed (Fig. 2). This indicated that the suppression of the high glucose-induced enhancement of contraction is not sufficiently explained by alteration of DG formation alone. Therefore, we hypothesized that the suppression might involve DG formation in addition to other mechanisms located in downstream relative to the DG signal in *ob/ob* mice.

To investigate this point, PKC activity in *ob/ob* mice was examined (Fig. 5B). The U46619-induced, calcium-dependent PKC activation in normal PSS was also detected in *ob/ob* mice; however, the

level was significantly lower than that in C57Bl mice. Similar challenges under high glucose conditions revealed that sub-maximal activation of PKC in the resting state detected in C57Bl mice was reduced whereas a slight increase was observed upon U46619 stimulation. Moreover, Rottlerin habited the PKC activity under high glucose condition. These changes in the PKC activity under high glucose conditions involved a calcium-independent PKC. We presumed that the high glucose-induced PKC activation was desensitized in *ob/ob* mouse PV; moreover, it might contribute to the suppression of the enhancement of the PV contraction (Scheme 2). PMA-induced activation of PKC was inhibited only in *ob/ob* mice (Fig. 5) supporting our position. Alteration of PKC activity in diabetic vascular cells has been reported by several groups (Koya and King, 1998; Park et al., 1999); however, the finding of a reduced glucose-dependence reduction in PKC is novel to our study.

The effects of a reduced glucose dependency of PKC activity on PI-turnover, was investigated in *ob/ob* mice in terms of total PI-turnover activity estimated via *myo*-inositol incorporation (Fig. 6). Inhibition of the U46619- activation of PI-turnover was detected under conditions identical to PKC desensitization. We hypothesized that the reduction of the glucose dependency of PKC might induce an inactivation of PI-turnover.

In the present study, we demonstrated that the blood glucose level (extracellular glucose level)-dependent enhancement of phasic contraction of PV in an NIDDM mouse model was suppressed under high glucose conditions. An alteration of the blood flow rate in OGTT (Table 2) supported this view. This dysfunction may reduce the blood supply to the liver as well as an increased PV pressure. A reduction of cellular DG formation from incorporated glucose appears to be one of the causes of this dysfunction. Moreover, it was suggested that the DG derived from glucose might be a different molecular species distinct from DG constructed from phosphatidylinositols by PLC by a calcium-independent PKC.

In the *ob/ob* mouse, it was found that the calcium-independent PKC was desensitized under high glucose conditions and associated with the dysfunction of PV contraction in diabetes.

In conclusion, PV contraction in a NIDDM mouse model was desensitized to increases in blood glucose levels. This alteration likely involves both decreased DG formation from glucose and a reduction of the glucose dependency of the calcium-independent PKC activation.

ACKNOWLEDGMENTS

This work was supported to in part by a Showa University Grant-in Aid for Innovative Collaborative Research Projects and a Special Research Grant-in Aid for Development of Characteristic Education from the Japanese Ministry of Education, Culture Sports, Science and Technology (K.N. & Y. S.).

JPET Fast Forward. Published on February 26, 2004 as DOI: 10.1124/jpet.103.062802
This article has not been copyedited and formatted. The final version may differ from this version.

REFERENCES

Babazono T, Kapor-Drezgic J, Dlugosz JA and Whiteside C (1998) Altered expression and subcellular localization of diacylglycerol-sensitive protein kinase C isoforms in diabetic rat glomerular cells. *Diabetes* **47**:668-676.

Chang AY and Schneider DI (1970) Abnormalities in hepatic enzyme activities during development of diabetes in db mice. *Diabetologia* **6**:274-278.

Chaudhuri A (2002) Vascular reactivity in diabetes mellitus. *Curr Diab Rep* **2**:305-310.

Coleman DL and Hummel KP (1967) Studies with the mutation, diabetes, in the mouse. *Diabetologia* **3**:238-248.

Conrad KP, Barrera SA, Friedman PA and Schmidt VM (1991) Evidence for attenuation of myo-inositol uptake, phosphoinositide turnover and inositol phosphate production in aortic vasculature of rats during pregnancy. *J Clin Invest* **87**:1700-1709.

Dawson RM, Irvine RF, Bray J and Quinn PJ (1984) Long-chain unsaturated diacylglycerols cause a perturbation in the structure of phospholipid bilayers rendering them susceptible to phospholipase attack. *Biochem Biophys Res Commun* **125**:836-842.

Desbuquois B and Aurbach GD (1971) Use of polyethylene glycol to separate free and antibody-bound peptide hormones in radioimmunoassays. *J Clin Endocrinol Metab* **33**:732-738.

Ganz MB and Seftel A (2000) Glucose-induced changes in protein kinase C and nitric oxide are prevented by vitamin E. *Am J Physiol Endocrinol Metab* **278**:E146-152.

Inoguchi T, Xia P, Kunisaki M, Higashi S, Feener EP and King GL (1994) Insulin's effect on protein kinase C and diacylglycerol induced by diabetes and glucose in vascular tissues. *Am J Physiol* **267**:E369-379.

Kanoh H, Yamada K, Sakane F and Imaizumi T (1989) Phosphorylation of diacylglycerol kinase in vitro by protein kinase C. *Biochem J* **258**:455-462.

Khan AH and Pessin JE (2002) Insulin regulation of glucose uptake: a complex interplay of intracellular signalling pathways. *Diabetologia* **45**:1475-1483.

Koya D and King GL (1998) Protein kinase C activation and the development of diabetic complications. *Diabetes* **47**:859-866.

Lee MW and Severson DL (1994) Signal transduction in vascular smooth muscle: diacylglycerol second messengers and PKC action. *Am J Physiol* **267**:C659-678.

Lee TS, Saltsman KA, Ohashi H and King GL (1989) Activation of protein kinase C by elevation of

glucose concentration: proposal for a mechanism in the development of diabetic vascular complications. *Proc Natl Acad Sci U S A* **86**:5141-5145.

MacMathuna PM (1992) Mechanisms and consequences of portal hypertension. *Drugs* **44**:1-13; discussion 70-12.

Mathis DR, Liu SS, Rodrigues BB and McNeill JH (2000) Effect of hypertension on the development of diabetic cardiomyopathy. *Can J Physiol Pharmacol* **78**:791-798.

Meyerovitch J, Backer JM and Kahn CR (1989) Hepatic phosphotyrosine phosphatase activity and its alterations in diabetic rats. *J Clin Invest* **84**:976-983.

Meyerovitch J, Rothenberg P, Shechter Y, Bonner-Weir S and Kahn CR (1991) Vanadate normalizes hyperglycemia in two mouse models of non-insulin-dependent diabetes mellitus. *J Clin Invest* **87**:1286-1294.

Miwa T, Endou M and Okumura F (1997) Prostaglandin E1 potentiation of the spontaneous phasic contraction of rat isolated portal vein by a cyclopiazonic acid-sensitive mechanism. *Br J Pharmacol* **120**:1419-1426.

Nobe K, Aizawa H, Ohata H and Momose K (1995) Protein kinase C is involved in translocation of diacyglycerol kinase induced by carbachol in guinea pig taenia coli. *Biochem Pharmacol* **50**:591-599.

Nobe K, Ohata H and Momose K (1993) Effect of diacylglycerol kinase inhibitor, R59022 on cytosolic free calcium level and force development in guinea pig taenia coli. *Res Commun Chem Pathol Pharmacol* **81**:331-343.

Nobe K, Ohata H and Momose K (1997) Receptor-mediated diacylglycerol kinase translocation dependent on both transient increase in the intracellular calcium concentration and modification by protein kinase C. *Biochem Pharmacol* **53**:1683-1694.

Nobe K, Sakai Y, Nobe H, Takashima J, Paul RJ and Momose K (2003) Enhancement effect under high-glucose conditions on U46619-induced spontaneous phasic contraction in mouse portal vein. *J Pharmacol Exp Ther* **304**:1129-1142.

Ozturk Y, Altan VM and Yildizoglu-Ari N (1996) Effects of experimental diabetes and insulin on smooth muscle functions. *Pharmacol Rev* **48**:69-112.

Park JY, Ha SW and King GL (1999) The role of protein kinase C activation in the pathogenesis of diabetic vascular complications. *Perit Dial Int* **19 Suppl 2**:S222-227.

Pillay TS and Makgoba MW (1991) Molecular mechanisms of insulin resistance. *S Afr Med J* **79**:607-613.

Rossi F, Grzeskowiak M, Della Bianca V and Sbarbati A (1991) De novo synthesis of diacylglycerol from

glucose. A new pathway of signal transduction in human neutrophils stimulated during phagocytosis of beta-glucan particles. *J Biol Chem* **266**:8034-8038.

Silva CL, Lenzi HL, Silva VF, Paulo FO and Noel F (2003) Cellular mechanisms involved in the increased contraction of portal veins from Schistosoma mansoni-infected mice. *Parasitol Res* **89**:16-22.

Szule JA, Fuller NL and Rand RP (2002) The effects of acyl chain length and saturation of diacylglycerols and phosphatidylcholines on membrane monolayer curvature. *Biophys J* **83**:977-984.

Vicario P, Brady EJ, Slater EE and Saperstein R (1987) Insulin receptor tyrosine kinase activity is unaltered in ob/ob and db/db mouse skeletal muscle membranes. *Life Sci* **41**:1233-1241.

Wakino S, Kintscher U, Liu Z, Kim S, Yin F, Ohba M, Kuroki T, Schonthal AH, Hsueh WA and Law RE (2001) Peroxisome proliferator-activated receptor gamma ligands inhibit mitogenic induction of p21(Cip1) by modulating the protein kinase Cdelta pathway in vascular smooth muscle cells. *J Biol Chem* **276**:47650-47657.

JPET Fast Forward. Published on February 26, 2004 as DOI: 10.1124/jpet.103.062802
This article has not been copyedited and formatted. The final version may differ from this version.

FIGURE LEGENDS

Table 1 Basic characteristics of experimental diabetic mice

Values in the C57Bl and *ob/ob* mice were obtained at 5-8 weeks of age. Oral glucose tolerance test was performed as described in Methods. Blood glucose levels were indicated in units of "mg/dL" and "(mM)". Blood insulin levels were also analyzed under fasting condition. *, $P<0.05$ vs C57Bl mouse.

Table 2 Alteration of blood cell movement in mouse PV

C57Bl and *ob/ob* mice were fasted for 12 hr (resting) or glucose treated (OGTT; 1 g/Kg body weight for 30 min). Subsequently, blood cell movement in PV was measured under conditions of ether anesthesia using a non-contact type laser Doppler blood flow meter. U46619-induced responses were detected with addition of 100 nM U46619 containing PSS for 5 min under anesthesia. Results are expressed as " % of resting level". *, $P<0.01$ vs resting level.

Table 3 Incorporation of [^{14}C]glucose into DG in diabetic mice

Isolated tissues were preincubated under normal and HG conditions, which included [^{14}C]glucose for 2 hr; subsequently, 100 nM U46619 was added for 5 min. Following termination of the response, radioactivity in the total DG fraction was quantified as described in Methods. Results are expressed as cpm/mg wet weight tissue. * $p<0.05$ vs. values in normal-PSS.

Fig. 1 Effects of HG-PSS treatment on U46619-induced contractile responses in mouse PV.

JPET Fast Forward. Published on February 26, 2004 as DOI: 10.1124/jpet.103.062802
This article has not been copyedited and formatted. The final version may differ from this version.

Representative experimental traces demonstrating the effect of U46619 (1-100 nM) on the contraction in the PV isolated from C57Bl(**A**) and *ob/ob* (**B**) mice. HG-PSS was pretreated 30 min prior to the U46619 stimulation.

Fig. 2 U46619 induced changes in amplitude (**A**) and the relationship between frequency and ON-time in C57Bl (**B**) and *ob/ob* (**C**) mice. Three parameters related to U46619-induced dose-dependent increase in phasic contraction were extracted from the data in Figure 1. The values of the three parameters were graphed in normal (circle)- and HG (square)-PSS in C57Bl (open) and *ob/ob* (closed) mice were plotted. Each concentration of U46619 (nM) is indicated in figures 2B and C as open (normal-PSS) and closed (HG-PSS) numbers. Each value represents the mean ± SEM from at least 12 independent determinations. * $p<0.05$ vs. normal-PSS. # $p<0.05$ vs. C57Bl mouse.

Fig. 3 Effect of long-term preincubation of portal vein under normal and high glucose conditions on U46619-induced contraction. PVs isolated from C57Bl (square) and *ob/ob* (circle) mice were incubated in normal (open) and high glucose (22.2 mM) PSS (closed) at 37^{o}C for indicated periods. During the preincubation, fresh normal and high glucose PSS were exchanged every 30 min, and both temperature and resting tension (1.2 mN) were maintained. After the preincubation, 30 nM U46619 was added for 10 min. Average of amplitude was calculated as same as Fig. 2A. Each value represents the mean ± SEM from 3 independent determinations. * $p<0.05$ vs. normal-PSS.

Fig. 4 U46619 induced changes in the total mass of DG in C57Bl (bright bars) and *ob/ob* (dark bars) mice PV. Tissues were preincubated in normal- and HG-PSS at 37 oC for 30 min. A phospholipase C

inhibitor (1 μM U73122) was introduced to several of these samples for the final 10 min of the preincubation; subsequently, 100 nM U46619 was added for 5 min. Following termination of the response, the total mass of DG was quantified as described in Methods. Results are expressed as ng/mg wet weight tissue. Each value represents the mean ± SEM from at least 5 independent determinations. * $p<0.05$ vs. resting level. # $p<0.05$ vs. 100 nM U46619 alone. † $p<0.05$ vs. normal-PSS.

Fig. 5 Response of PKC activity in U46619-treated C57Bl (**A**) and *ob/ob* (**B**) mice PV. Fresh tissues were preincubated in normal- and HG-PSS at 37 ^{o}C for 30 min. These samples were exposed to 1 μM U73122 (U73), 1 μM calphostin C (Cal-C), 1 μM Gö6976 (Gö) or 1 μM Rottlerin (Rott) for 5 min; subsequently, 100 nM U46619 was added for the 5 min. PMA (3 μM) was singly treated for 5 min. These treatments were terminated and membrane fractions were collected as described in "Methods". PKC activity in each sample was assayed with an Amersham PKC-assay kit. Results are expressed as pmol/min/mg protein. Each value represents the mean ± SEM of at least 5 independent determinations. * $p<0.01$ vs. resting and # $p<0.01$ vs. U46619 alone.

Fig. 6 Effects of U73122 on U46619-induced [^{3}H]*myo*-inositol in C57Bl (bright bars) and *ob/ob* (dark bars) mice PV. [^{3}H]*myo*-inositol pre-labeled tissues were preincubated in normal- and HG-PSS for 30 min, followed by incubation in the presence or absence of 1 μM U73122 for 5 min; subsequently, 100 nM U73122 was added for 5 min. Upon termination of these treatments; the radioactivity of [^{3}H]phosphoinositides was measured as described in "Methods". Each value represents the mean ± SEM. of at least 5 independent determinations. * $p<0.05$ vs resting level. # $p<0.05$ vs U46619 alone.

Schemes Alterations of glucose derived DG formation and PKC activation in C57Bl (A) and *ob/ob* (B) mice. U46619-induced alterations of the DG-PKC pathway under high glucose conditions are illustrated. Abbreviations in the schemes with; Cal-C, calphostin C; DG, diacylglycerol; GLT, glucose transporter; Ins-R, insulin receptor; PLC, phospholipase C.

JPET Fast Forward. Published on February 26, 2004 as DOI: 10.1124/jpet.103.062802
This article has not been copyedited and formatted. The final version may differ from this version.

Table 1 Basic data of experimental diabetic mice

Experimental Groups	Animals	Body weight (g)	Blood glucose (mg/dL)		Insulin level (μU/mL)
			Fasting	OGTT	
C57Bl	6	34.0 ± 2.0	164.0 ± 11.2 (9.10 ± 0.62 mM)	234.5 ± 15.0 (13.02 ± 0.83 mM)	40.5 ± 1.9
ob/ob	6	48.0 ± 2.4 *	397.8 ± 11.7* (22.08 ± 0.65 mM)	445.7 ± 9.2* (24.74 ± 0.51 mM)	179.7 ± 7.9 *

Table 1

JPET Fast Forward. Published on February 26, 2004 as DOI: 10.1124/jpet.103.062802
This article has not been copyedited and formatted. The final version may differ from this version.

Table 2 Alteration of blood cell movement inmouse portal vein

Experimental Groups	Animals	Blood cell movement (% of resitng level)	
		OGTT (30 min)	100 nM U46619
C57Bl	5	142.91 ± 3.73*	36.73 ± 2.87*
ob/ob	5	100.27 ± 1.70	38.65 ± 8.51*

Table 2

JPET Fast Forward. Published on February 26, 2004 as DOI: 10.1124/jpet.103.062802
This article has not been copyedited and formatted. The final version may differ from this version.

Table 3 Incorporation of [^{14}C]glucose into DG in diabetic mice

Experimental Groups	Treatments	Animals	[^{14}C] DG (cpm/mg wet wt.)		% of Normal-PSS
			Normal-PSS	HG-PSS	
C57Bl	Resting	5	383.6 ± 38.0	790.4 ± 60.2*	213.0
	U46619	5	426.8 ± 46.6	807.4 ± 58.8*	202.4
ob/ob	Resting	5	364.2 ± 12.0	518.2 ± 16.0*	143.0
	U46619	5	362.4 ± 7.7	522.2 ± 29.7*	143.7

Table 3

JPET Fast Forward. Published on February 26, 2004 as DOI: 10.1124/jpet.103.062802
This article has not been copyedited and formatted. The final version may differ from this version.

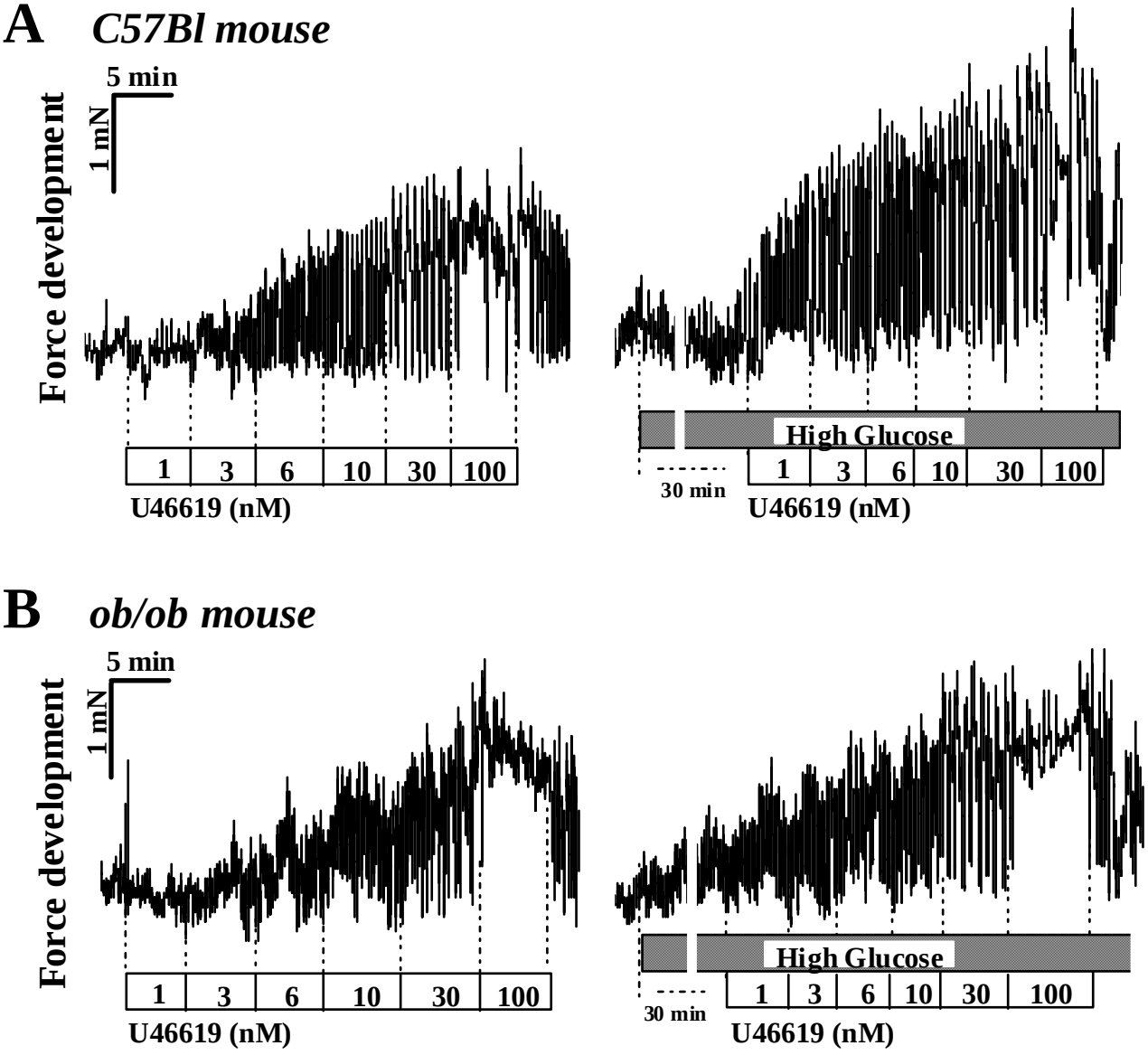

Fig. 1

JPET Fast Forward. Published on February 26, 2004 as DOI: 10.1124/jpet.103.062802
This article has not been copyedited and formatted. The final version may differ from this version.

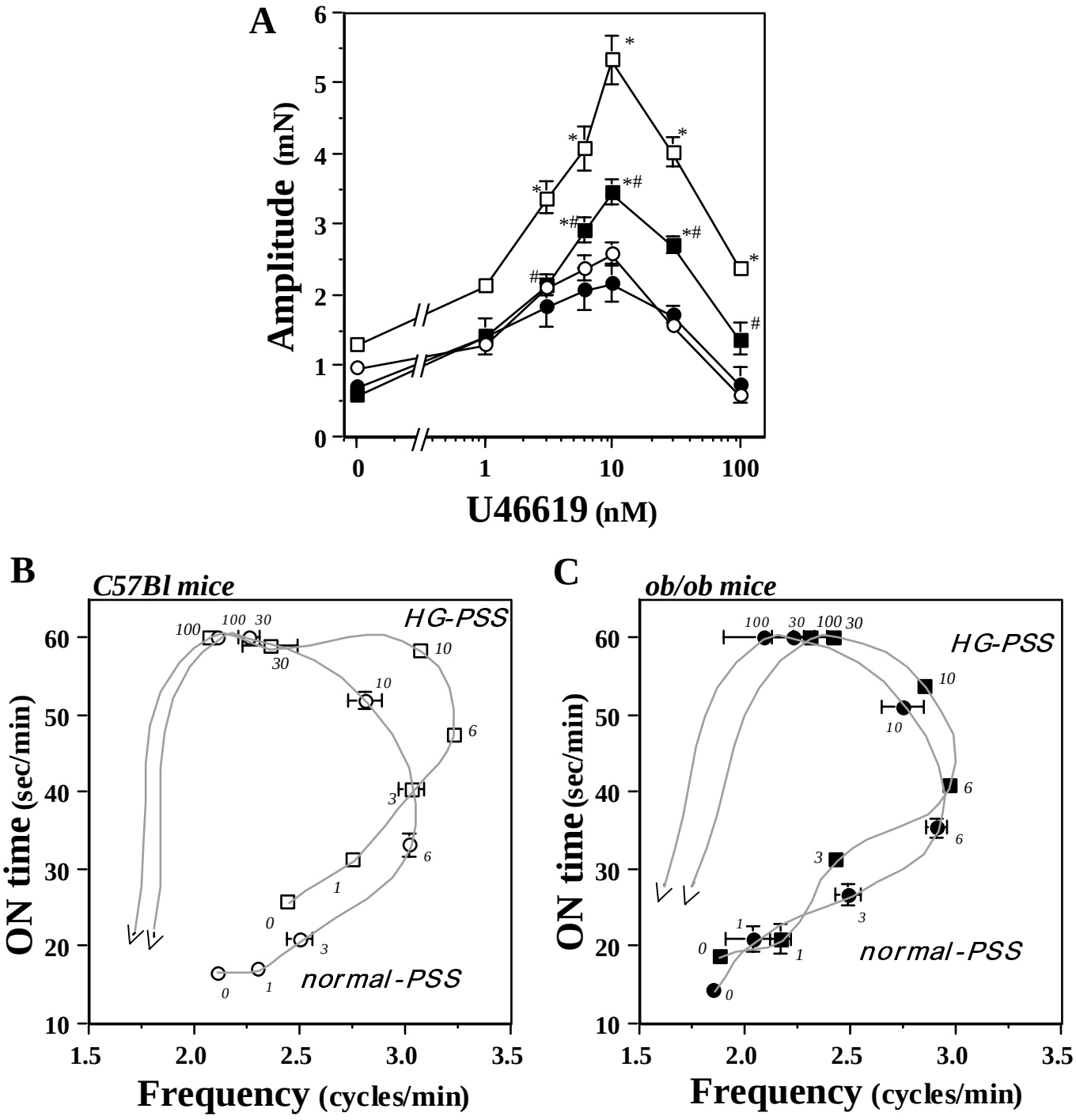

Fig. 2

JPET Fast Forward. Published on February 26, 2004 as DOI: 10.1124/jpet.103.062802
This article has not been copyedited and formatted. The final version may differ from this version.

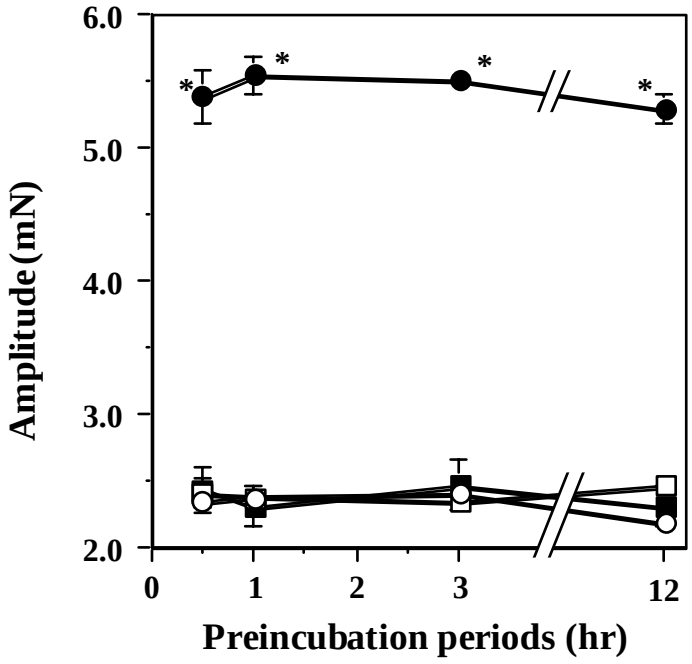

Fig. 3

JPET Fast Forward. Published on February 26, 2004 as DOI: 10.1124/jpet.103.062802
This article has not been copyedited and formatted. The final version may differ from this version.

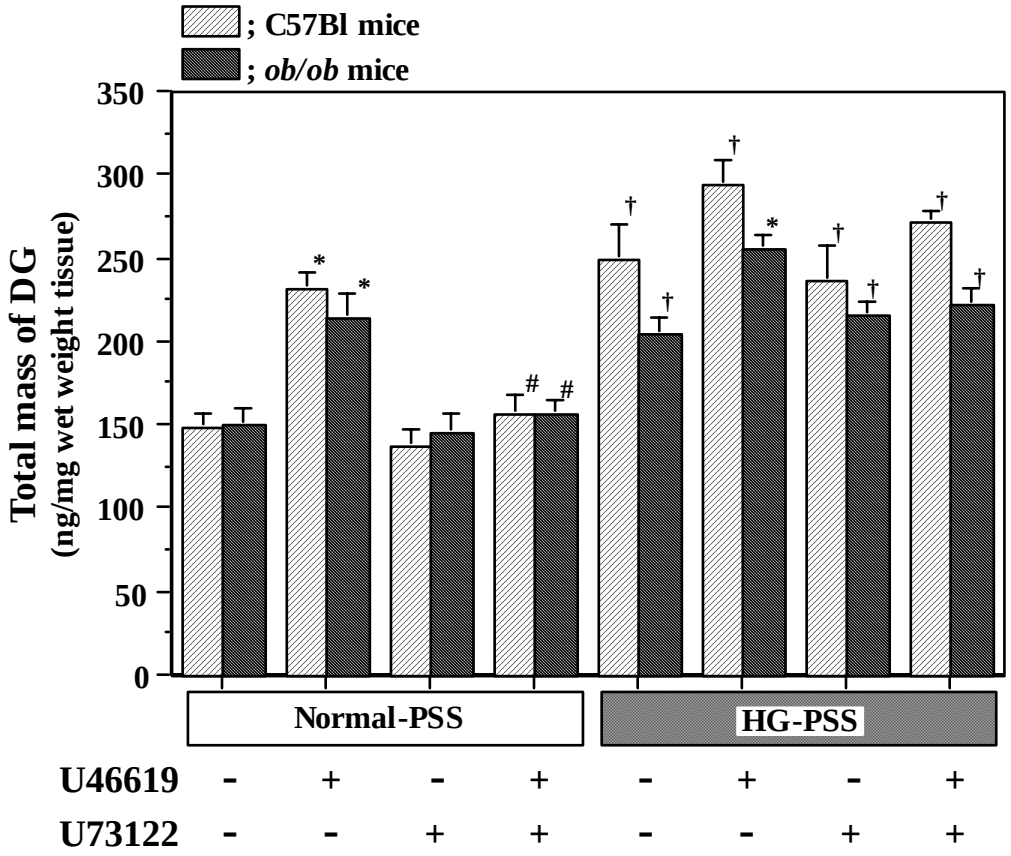

Fig. 4

JPET Fast Forward. Published on February 26, 2004 as DOI: 10.1124/jpet.103.062802
This article has not been copyedited and formatted. The final version may differ from this version.

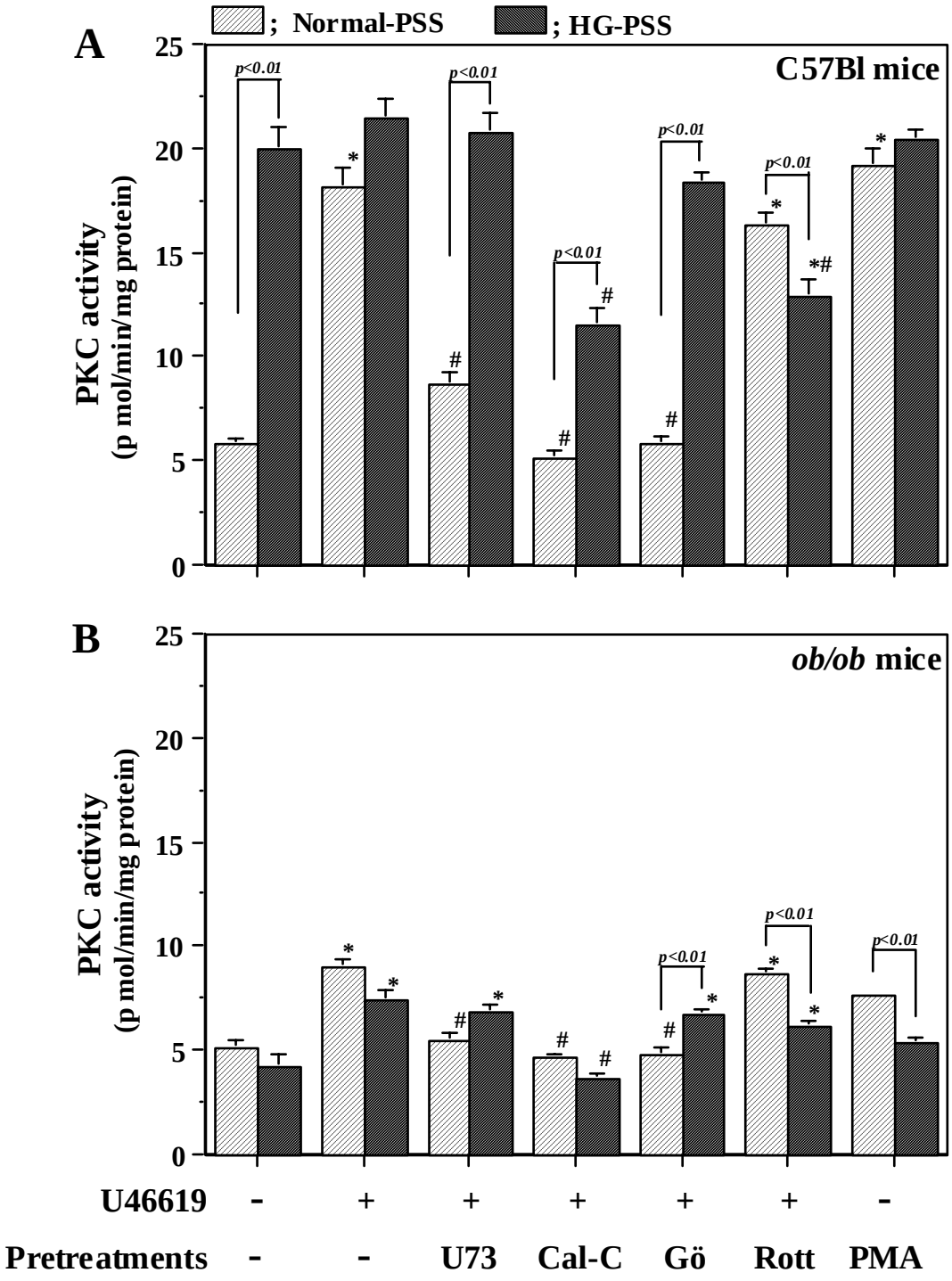

Fig. 5

JPET Fast Forward. Published on February 26, 2004 as DOI: 10.1124/jpet.103.062802
This article has not been copyedited and formatted. The final version may differ from this version.

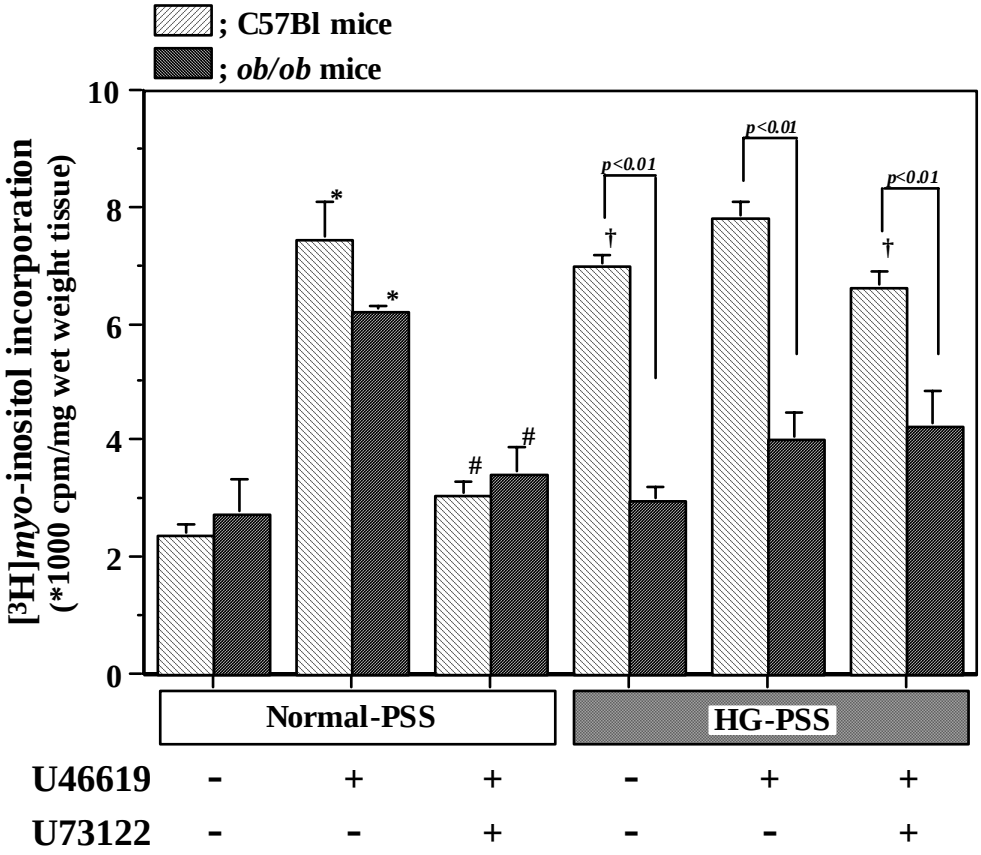

Fig. 6

JPET Fast Forward. Published on February 26, 2004 as DOI: 10.1124/jpet.103.062802
This article has not been copyedited and formatted. The final version may differ from this version.

A: C57Bl mouse portal vein in HG-PSS

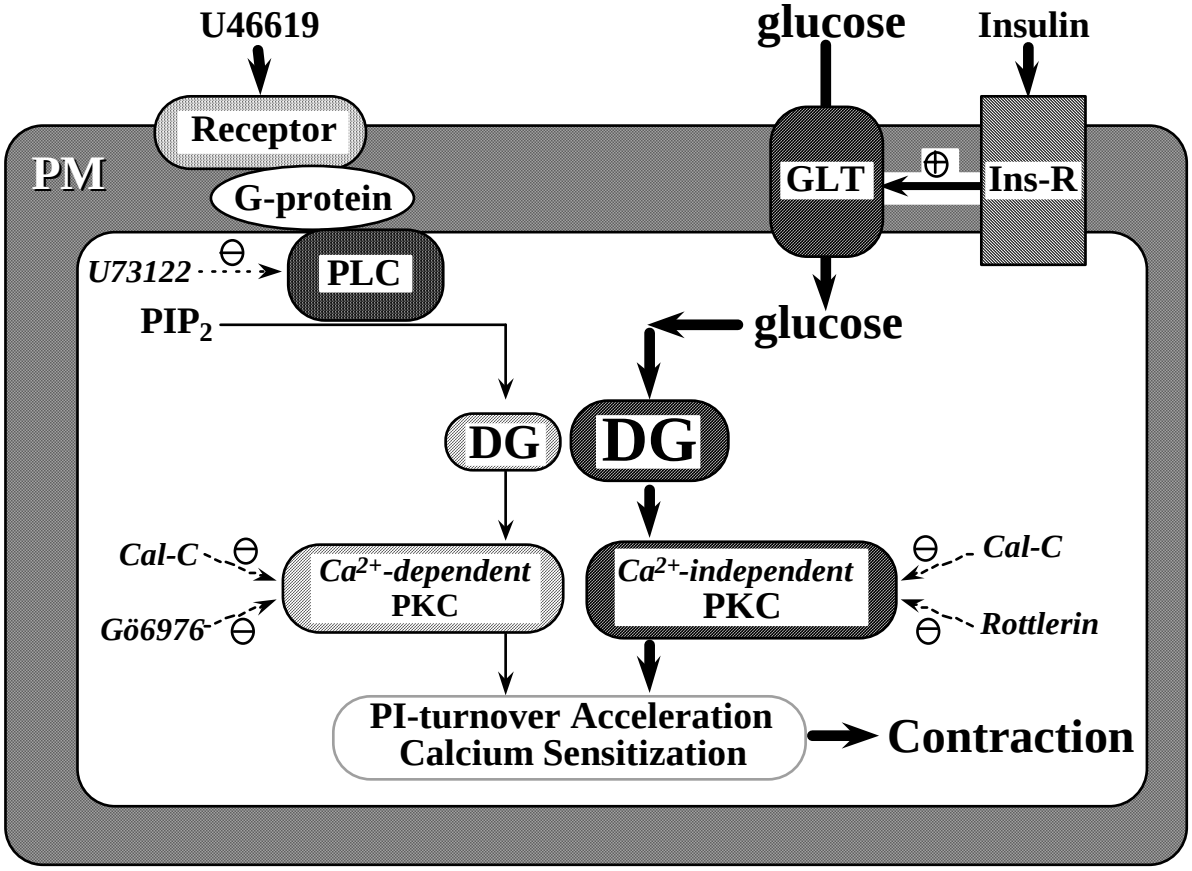

B: *ob/ob* mouse portal vein in HG-PSS